IF-UFRJ-93-03

INSTITUTO DE FISICA

Fermilab Library
0 1160 0017945 1

IF/UFRJ/93/03

16

BLOCK COPOLYMERS AND THE VISUAL CORTEX

M. Bahiana and C. Cortez-Maghelly
Rio de Janeiro U. Rio de Janeiro State U.

June/93

UNIVERSIDADE FEDERAL DO RIO DE JANEIRO
INSTITUTO DE FÍSICA
Cx. P. 68.528
21.944 - RIO DE JANEIRO
BRASIL

FERMILAB
JUL 27 1993
LIBRARY

Block Copolymers and the Visual Cortex

M. Bahiana
Universidade Federal do Rio de Janeiro
Instituto de Física, Departamento de Física dos Sólidos
21945-970, Rio de Janeiro, RJ Brazil

C. Cortez-Maghelly
Universidade do Estado do Rio de Janeiro
Instituto de Biologia, Departamento de Fisiologia
20560, Rio de Janeiro, RJ, Brazil

June 7, 1993 Rio de Janeiro State U.

Abstract

The similarity between striped patterns found in different systems motivates a comparison between a model for the lamellar pattern of block copolymers and a model for the ocular dominance pattern in the primary visual cortex.

T

1 Introduction

The main purpose of this paper is to compare two problems which are apparently different: the formation of the ocular dominance (OD) stripes in layer IVc of the primary visual cortex of mammals and the microphase separation of diblock copolymers. The link between these problems is the equilibrium pattern consisting of locally ordered stripes with Y and H type bifurcations. Actually there are several systems in nature that exhibit the same kind of pattern, for example: the zebra skin and our fingerprints, which are equilibrium patterns, and the convection in a Rayleigh-Bénard cell (Greenside & Coughran 1984), a nonequilibrium pattern formed by rolls of upward- and downward-moving regions of fluid. We hope that if the pattern can be obtained from a model which is free of details, it can be used to describe many

different systems with the correct identification of parameters. We have chosen to analyze the block copolymer (BCP) and the visual cortex problems because these systems have been studied independently with the aid of computer simulations (Swindale 1980,1982, Swindale *et al* 1987, Oono & Bahiana 1988,1989, Bahiana & Oono 1990) .

Light coming from objects are translated by the retina into nerve impulses which are carried over the optic nerve to the brain. The primary target of this nerve are the geniculate bodies. The optic nerve transmits signals from the right side of the visual field to the lateral geniculate body in the left hemisphere, and it transmits signals from the left side of the visual field to the right hemisphere. The lateral geniculate bodies then relay the signals to the occipital lobe on the same side of the brain, and specifically to the primary visual cortex, which does an initial analysis of the image and transmits selected information about it to other regions of the brain. By injecting a tracer in one of the eyes it is possible to map regions receiving input from one particular eye (Hubel & Wiesel 1977, Hubel *et al* 1978, Gosh & Shatz 1992, Meissirel *et al* 1991). The visual pathways from the left and right eyes to the cortex are segregated within layer IVc of the visual cortex into a pattern of OD (Hubel & Wiesel 1977, Toot *et al* 1988, Blakemore & Price 1987, Matsubara *et al* 1985, Lowel & Singer 1990). This pattern consists of meandering stripes corresponding to left and right eye-dominant regions alternating with periodicity of 700-800 μm (Swindale 1980,1992), as can be seen in Fig. 1. It has been suggested (Callaway & Katz 1991) that the development of this orientation-specific circuitry may depend on temporal correlation of activity for regulation of axonal rearrangements. Experiments have demonstrated that synapses (Swindale 1980, Bakkum *et al* 1991) affect the growth of other synapses through an interaction that varies in magnitude and signal within a distance of $600\mu m$.

A diblock copolymer is a linear-chain molecule consisting of two subchains, a and b, grafted covalently to each other (Burke & Weiss 1973). Polystyrene-polybutadiene and polystyrene-polyisoprene are the most frequent examples in the literature (for example, see Hashimoto *et al* 1986 and Inoue *et al* 1969). The subchains a and b are made of different monomer units, A and B respectively. In polymer systems even a weak repulsion between unlike monomers A and B induces a strong repulsion between a and b. As a result, the different subchains tend to segregate below some temperature T_c, but, as they are chemically bonded, even a complete segregation of subchains a and b cannot lead to a macroscopic phase separation as in mixtures of two homopolymers. Only a local microphase separation occurs: microdomains rich in A or B are formed generating a striped pattern if sub-

chains have similar lengths (Shibayama *et al* 1983) (see Fig. 2).

The patterns in figures 1 and 2 are quite similar altough reflecting order at different length scales: stripes in the cortex pattern are hundreds of μm wide, while for BCP they are hundreds of $\AA$ wide. As will be seen below, patterns generated by computer simulations in both cases are indistinguishble. We try to link these problems by comparing the models used for the simulations. The model proposed by Swindale for the formation of OD stripes is reviewed in Section 2. In Section 3 we summarize the cell dynamical system (CDS) model for the BCP microphase separation. Section 4 shows a comparison between the two models.

2 A model for the ocular dominance stripes

Swindale (Swindale 1980) has proposed a model in which the effects that a synapse exerts on the growth of other synapses are not local, but extend over space, varying both in magnitude and sign. Synapses of one eye compete among themselves, so that a local excess of one eye type will encourage further local growth of synapses of that type, but will discourage the growth of similar synapses if they are more than 200μm distant. The cortex is regarded as a two-dimensional sheet of tissue; $n_R(\vec{r})$ and $n_L(\vec{r})$ are the densities of right and left eye synapses respectively at a position $\vec{r}$ on the cortical surface. the rate of growth at a point in the cortex is then written as a locally weighted sum of the surrounding $n_r(\vec{r})$ and $n_L(\vec{r})$. The interactions among synapses can be R-R, R-L, L-L and L-R, where R stands for right and L for left eye. The corresponding weights w_{RR} and w_{LL} are positive for short distances (0-200μm)and negative for larger ones (200-600μm), while w_{RL} and w_{LR} have the opposite behavior. The general form of these functions is:

$$w(r) = C_1 \exp(-r^2/d_1) - C_2 \exp\{-(r-h)^2/d_2\} \tag{2.1}$$

where r is the radial distance in units of 100μm and C_1, C_2, d_1, d_2 and h are constants. The rate of growth for, e.g., n_R is given by:

$$\frac{\partial n_R}{\partial t} = s_R f(n_r), \tag{2.2}$$

where the function f prevents n_R and n_L from being negative and establish an upper limit, N, to their density in the cortex. A possible form for f is $f(n_R) = n_R(N - n_R)$. For most computations it is assumed that the sum of the densities of left and right eyes is constant throughout the cortex: $n_R + n_L = N$ everywhere. in this case the pattern formation can be described by a single

variable $\varphi = n_R - n_L$ ranging from $-N$ to N. From this incompressibility condition the equations above are reduced to:

$$\frac{\partial \varphi}{\partial t} = (\varphi * w + K)(N - \varphi)(N + \varphi), \tag{2.3}$$

with $w = w_{RR} + w_{LL} (= -w_{RL} - w_{LR})$ and $K = N * (w_{RR} - w_{LL})$. If both eyes are equivalent, then $K = 0$. The symbol $*$ stands for convolution. The pattern obtained from equation (2.3) can be seen in Fig. 3.

In the above pattern, both eyes compete equally producing black and white stripes with the same width. It is known from experience (Hubel *et al* 1978, Callaway & Katz 1991) that if one of the eyes is closed or removed shortly after birth, that is, during the period of OD pattern formation, the final pattern will be altered. The stripe corresponding to the deprived eye will be narrower. The effect of monocular deprivation is mimicked by Swindale by choosing $K \neq 0$ in (2.3) after some period of time, while creating an anysotropy in order to induce the formation of stripes. With isotropic conditions, the pattern consists of circular islands corresponding to the deprived eye on a background corresponding to the predominant eye.

3 Cell dynamical system model for block copolymers

The cell dynamical system (CDS) provides a computationally efficient model for phase ordering processes. It was first proposed by Oono and Puri (Oono & Puri 1987,1988) to simulate the process of spinodal decomposition, which is briefly described below.

Spinodal decomposition is the process by which an unstable phase undergoes phase separation (Gunton *et al* 1983). The phase separation dynamics of two species, A and B, can be described in terms of the time-dependent local number densities $\psi_A(\vec{r},t)$ and $\psi_B(\vec{r},t)$. If the system is incompressible $\psi_A + \psi_B = 1$ everywhere. In this case an order parameter is defined as $\psi(\vec{r},t) = \psi_A(\vec{r},t) - \psi_B(\vec{r},t)$. $\psi = 0$ represents the homogeneous phase, if $\psi(\vec{r},t) > 0 (< 0)$ there is a predominance of $A(B)$. Below a certain temperature, T_c, thermodynamic equilibrium corresponds to a coexistence of two phases, one rich in A (e.g. ψ_α), the other poor in this species (e.g. ψ_β). This equilibrium situation is given by the condition $\mu_A = \mu_B$ where μ is the chemical potential which defines the coexistence curve. The process of phase separation itself will depend on the initial stability of the phases. States for which $(\partial\mu/\partial\psi) > 0 (< 0)$ are termed metastable (unstable) and

are nonequilibrium states. Unstable states will phase separate by spinodal decomposition, while metastable states will phase separate by nucleation. In the spinodal decomposition process no activation energy is required for the system to begin to phase separate. In contrast to nucleation in which a localized droplet of finite size is required to initiate phase separation, the initial process is manifested as a finely dispersed precipitate which gradually coarsens forming an interconnected pattern.

In the CDS model space and time are discrete, so that the order parameter is written as $\psi(t,n)$ where n refers to the center of cell n. The dynamics of each cell is described by:

$$\psi(t+1,n) = \mathcal{F}(\psi(t,n)). \tag{3.4}$$

The form of $\mathcal{F}$ depends on the kind of dynamics to be described. For spinodal decomposition the map $\mathcal{F}$ has a flow with a single hyperbolic unstable fixed point (the unstable homogeneous phase)and two hyperbolic stable fixed points symmetrically located on each side of the unstable fixed point (the stable phases). The exact form of $\mathcal{F}$ is not important for the late stage behavior, as was demonstrated in (Oono & Puri 1987). Here $\mathcal{F}(\psi) = \mathcal{A}\tanh(\psi(t,n))$ has been chosen. Above the critical temperature $\mathcal{A} < 1$, and below $\mathcal{A} > 1$.

The interaction with the other cells results in a driving force on the order parameter proportional to its difference from the average of the order parameter in the neighboring cells, resulting in a coupling of the form:

$$\psi(t+1,n) = \mathcal{F}(\psi(t,n)) + \mathcal{D}\left[\langle\langle\psi(t,n)\rangle\rangle - \psi(t,n)\right], \tag{3.5}$$

where $\mathcal{D}$ is a positive constant proportional to the diffusion constant, and $\langle\langle * \rangle\rangle$ is the isotropic spatial average. For a 2-dimensional square lattice, we choose:

$$\begin{aligned}\langle\langle\psi(t,n)\rangle\rangle &= \frac{1}{6}\sum(\psi \text{ in the nearest neighbor cells}) + \\ &\quad \frac{1}{12}\sum(\psi \text{ in the next nearest neighbor cells}).\end{aligned} \tag{3.6}$$

If the conservation of $\psi(t,n)$ is enforced locally, we have:

$$\psi(t+1,n) = \psi(t,n) + \mathcal{I}(t,n) - \langle\langle\mathcal{I}(t,n)\rangle\rangle \tag{3.7}$$

with

$$\mathcal{I}(t,n) \equiv \mathcal{F}(\psi(t,n)) + \mathcal{D}\left[\langle\langle\psi(t,n)\rangle\rangle - \psi(t,n)\right] - \psi(t,n). \tag{3.8}$$

To construct a CDS model of BCP, the strategy was to find the minimum modification of the above CDS model for spinodal decomposition. In ordinary

spinodal decomposition the domain size increases indefinitely. In contrast, the domain growth of BCP is limited by the covalent bond between subchains a and b. In other words, the state with $\psi = 0$ becomes more stable than that with $\psi \neq 0$ when there is no spatial gradient. The simplest way to take this into account is to modify (3.7) as follows (Oono & Shiwa 1987):

$$\psi(t+1,n) = (1-\mathcal{B})\psi(t,n) + \mathcal{I}(n,t) - \langle\langle\mathcal{I}(n,t)\rangle\rangle, \tag{3.9}$$

where B is a small positive number. In a large bulk cluster, ψ is spatially uniform, so that $\mathcal{I}$ and its local average $\langle\langle\mathcal{I}\rangle\rangle$ become identical. Hence, in the bulk phase (3.9) simply reads $\psi(t+1,n) = (1-\mathcal{B})\psi(t,n)$, which has the fixed point at $\psi = 0$.

For uneven BCP, the necessary minimal modification to (3.9) is to stabilize an appropriate local concentration compatible with the subchain size fraction. Let f be the ratio between the length of the shorter subchain and the total chain length. In this case we should stabilize $\psi = 1-2f$ instead of $\psi = 0$, so that we obtain

$$\psi(t+1,n) = \psi(t,n) - \mathcal{B}\left(\psi(t,n) - 1 + 2f\right) + \mathcal{I}(t,n) - \langle\langle\mathcal{I}(t,n)\rangle\rangle. \tag{3.10}$$

The choice of parameters $\mathcal{A}$, $\mathcal{D}$ and $\mathcal{B}$ must be such that initial fluctuations of ψ are amplified and we obtain a $\psi \neq 0$ as the final state. Linearizing (3.10) about the $\psi = 1-2f$ solution we get

$$\delta(n,t+1) = (1-\mathcal{B})\delta(n,t) - \tilde{\Delta}[\mathcal{A}(1-\tanh^2(1-2f))\delta(n,t) - \delta(n,t)] - \mathcal{D}\tilde{\Delta}^2\delta(n,t) \tag{3.11}$$

where $\delta(n,t) = \psi(t,n) - (1-2f)$ and $\tilde{\Delta}$ is the discrete Laplacian: $\tilde{\Delta}\bullet \equiv \langle\langle\bullet\rangle\rangle - \bullet$. Applying a discrete Fourier transform to both sides of this equation yields

$$\begin{aligned}\frac{\delta(k,t+1)}{\delta(k,t)} &= \\ &1 - \mathcal{B} - \left[\mathcal{A}\left(1-\tanh^2(1-2f)\right) - 1\right] E(k_x,k_y) - \mathcal{D}E(k_x,k_y)^2\end{aligned} \tag{3.12}$$

where

$$E(k_x,k_y) = \frac{1}{3}(\cos k_x + \cos k_y + \cos k_x \cos k_y) - 1. \tag{3.13}$$

Stability of the homogeneous solution is given by the condition $|\delta(k,t+1)| < |\delta(k,t)|$. For even BCP ($f = 1/2$) the condition for obtaining a lamellar pattern, that is, for the $\psi = 0$ solution being unstable is:

$$\mathcal{B} \leq \frac{(\mathcal{A}-1)^2}{4\mathcal{D}} \tag{3.14}$$

Here we fix $\mathcal{D}$=0.5 and $\mathcal{A} = 1.3$ so that $\mathcal{B} \leq 0.045$ generates a pattern. Fig. 4 shows patterns obtained from (3.9) in this region of parameters.

4 Discussion

The similarity between patterns in figures 1 and 2 clearly shows that both systems should admit the same mathematical description. Swindale's model provides a continuous description with six parameters. The CDS model is discrete from the beginning, which is more adequate since the main purpose is to simulate the equilibrium pattern. A model based on a partial differential equation must be discretized in order to be numerically integrated and becomes a , usually inefficient, discrete model which may even present a chaotic behavior. Also the CDS model requires two parameters less and, in practice, we keep $\mathcal{D}$ and $\mathcal{A}$ fixed and work only with $\mathcal{B}$ and f. The average stripe width scale as $\mathcal{B}^{-\theta}$, $\theta > 0$ and the parameter $\mathcal{B}$ is found to be related to the polimerization index N as $\mathcal{B} \sim N^{-2}$(Oono & Bahiana 1988). We expect to find a similar relation for the visual cortex problem. We suggest the following mapping between the models:

visual cortex	BCP
$n_{R(L)}$	$\psi_{A(B)}$
$\varphi(\vec{r}, t)$	$\psi(t, n)$
monocular deprivation	uneven BCP

The main difference between the models is that conservation of φ is not imposed in Swindale's formulation. We believe that this fact is crucial for the monocular deprivation effect. In the CDS model, the pattern responds to changes from even to uneven molecule (and vice-versa) at any time. This apparently does not happen in Swindale's model; the parameter K must be altered in the beginning of the simulation in order to change the relative stripe width. Nevertheless, we consider that the energy functionals for both models belong to the same universality class.

Acknowledgements

One of us (MB) was partially supported by CNPq (Brazil).

References

M. Bahiana and Y. Oono. Cell dynamical system approach to block copolymers. *Phys. Rev. A*, **41**,6763, 1990.

B. W. Bakkum, L. A. Benevento, and R. S. Cohen. Effects of light/dark and dark rearing on synaptic morphology in the superior colliculus and visual cortex of the postnatal and adult rat. *J. Neurosci. Res.*, **28**, 65, 1991.

C. Blakemore and D. J. Price. The organization and post-natal development of area 18 of the cat's visual cortex. *J. Physiol.*,**384**, 263, 1987.

J. J. Burke and V. Weiss, editors. *Block and Graft Copolymers.* Syracuse University Press, Syracuse, NY, 1973.

E. M. Callaway and L. C. Katz. Effects of binocular deprivation on the development of clustered horizontal connections in cat striate cortex. *Proc. Natl. Acad. Sci. USA*, **88**, 745, 1991.

A. Gosh and C. J. Shatz. Pathfinding and target selection by developing geniculocortical axons. *J. Neurosci.*, **12**, 39, 1992.

H. S. Greenside and W. M. Coughran. Nonlinear pattern formation near the onset of Rayleigh-Bènard convection. *Phys. Rev. A*, **30**,398, 1984.

J. D. Gunton, M. San Miguel, and P. S. Sahini. In C. Domb and J. L. Lebowitz, editors, *Phase Transitions and Critical Phenomena*, volume 8, page 269. Academic Press, New York, 1983.

T. Hashimoto, K. Kowasaka, M. Shibayama, and S. Suehiro. Time-resolved small-angle x-ray scattering studies on the kinetics of the order- disorder transition of block copolymers. 1. Experimental technique. *Macromolecules*, **19**,750, 1986.

D. H. Hubel and T. N. Wiesel. Functional architeture of macaque monkey visual cortex. *Proc. R. Soc. Lond. B*, **198**, 1, 1977.

D. H. Hubel, T. N. Wiesel, and M. P. Stryker. Anatomical demontration of orientation columns in macaque monkey. *J. Comp. Neur.*, **177**, 361, 1978.

T. Inoue, T. Soen, T. Hashimoto, and H. Kaway. Thermodynamic interpretation of domain structure in solvent-cast films of a-b type block copolymers of styrene and isoprene. *J. Pol. Sci. A-2*, **7**, 1283, 1969.

S. Lowel and W. Singer. Tangencial intracortical pathways and the development of iso-orientation bands in cat striate cortex. *Brain Res.*, **56**, 99, 1990.

J. Matsubara, M. Cynader, N. V. Swindale, and M. P. Stryker. Intrisic projections within visual cortex: evidence for orientation-specific local connections. *Proc. Natl. Acad. Sci. USA*, **82**, 935, 1985.

C. Meissirel, C. Dehay, M. Berland, and H. Kennedy. Segregation of callosal and association pathways during development in the visual cortex of the primate. *J. Neurosci.*, **11**, 3297, 1991.

Y. Oono and M. Bahiana. $\frac{2}{3}$-power law for copolymer lamellar thickness implies a $\frac{1}{3}$ power law for spinodal decomposition. *Phys. Rev. Lett.*, **61**, 1109, 1988.

Y. Oono and M. Bahiana. Block copolymer lamellar thickness: an exactly solvable model. *J. Phys.: Condens. Matter*, **1**, 529[illegible]

Y. Oono and S. Puri. Computationally efficient modeling of ordering of

quenched phases. *Phys. Rev. Lett.*, **58**, 863, 1987.
Y. Oono and S. Puri. Study of phase separation dynamics by use of cell dynamical systems. i.Modeling. *Phys. Rev. A*, **38**, 434, 1988.
Y. Oono and Y. Shiwa. Computationally efficient modeling of block copolymer and Bènard pattern formation. *Mod. Phys. Lett. B*, **1**, 49, 1987.
M. Shibayama, T. Hashimoto, and H. Kawai. Ordered structure in block polymer solutions. 5. Equilibrium and nonequilibrium aspects of microdomain formation. *Macromolecules*, **16**, 1434, 1983.
N. V. Swindale. A model for the formation of ocular dominance stripes. *Proc. R. Soc. Lond. B*, **208**, 243, 1980.
N. V. Swindale. A model for the formation of orientation columns. *Proc. R. Soc. Lond. B*, **215**, 211, 1982.
N. V. Swindale. A model for the coordinated development of columnar systems in primate striate cortex. *Biol. Cybern.*, **66**, 217, 1992.
N. V. Swindale, J. A. Matsubara, and M. S. Cynader. Surface organization of orientation and direction selectivity in cat area 18. *J. Neurosci.*, **7**, 1414, 1987.
R. B. Tootell, S. L. Hamilton, M. S. Silverman, and E. Swithers. Functional anatomy of macaque monkey striate cortex. i. Ocular dominance, binocular interactions, and baseline conditions. *J. Neurosci.*, **8**, 1500, 1988.
T. A. Witten. Structured fluids. *Physics Today*, **43**, 21, 1990.

Figure Captions

Figure 1 A reconstruction of the pattern of OD stripes in area 17 of a macaque. Regions receiving input from one eye are shaded black in the figure; the unshaded areas between the stripes receive their input from the other eye (Taken from Swindale (1980)).

Figure 2 A block copolymer pattern obtained after precipitation and further evaporation of the solvent.The two polymer species in each copolymer molecule appear as dark and light stripes of 400$\AA$ of width.(Taken from (Witten 1990)).

Figure 3 The pattern obtained after 160 iterations of equation (2.3) with $K = 0$, $C_1 = 0.3$, $C_2 = 1.0$, $d_1 = 5.0$, $d_2 = 1.4$ and $h = 3.7$. This choice of parameters corresponds to a symetric behaviour of right and left eyes. A point is displayed wherever the input from a given eye predominates over the other.The initial condition is a random distribution of inputs from both eyes. (Taken from (Swindale 1980)).

Figure 4 The pattern obtained from equation (3.10) after 500 iterations. The initial condition is ψ uniformly distributed in the interval [-0.05,+0.05]. Here we use $\mathcal{A} = 1.3$, $\mathcal{D} = 0.5$ f=0.5 (which means equal chain lengths for both polymers in the BCP molecule), $\mathcal{B} = 0.02$ and periodic boundary conditions. The points represent lattice sites in which $\psi > 0$, that is, in which there is a predominance of A. This pattern should be compared with the one in Fig. 3.

Figure 5 The pattern for an uneven molecule and isotropic conditions. The conditions in this simulation are the same as in figure 4, exept that here $f = 0.35$. Instead of stripes we observe nearly circular island of the minority species in a matrix of the majority species.

Figure 6 The pattern for an uneven molecule but in a anysotropic lattice. The simulation parameters are the same as in figure 5. The anysotropy forces the formation of stripes of different widths.

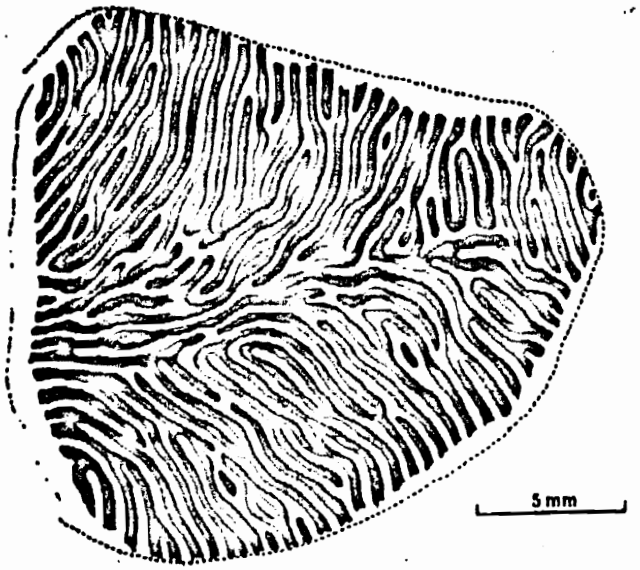

FIGURE 1

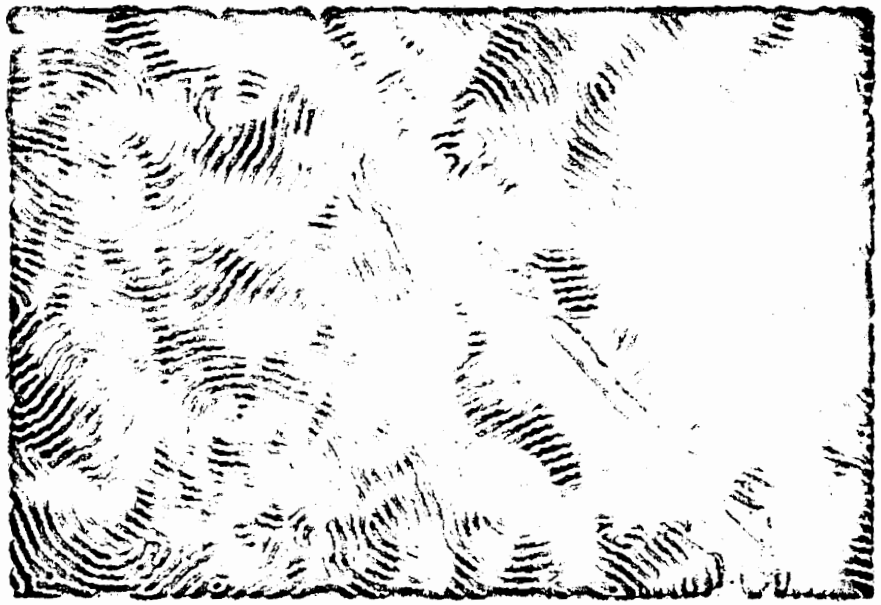

FIGURE 2

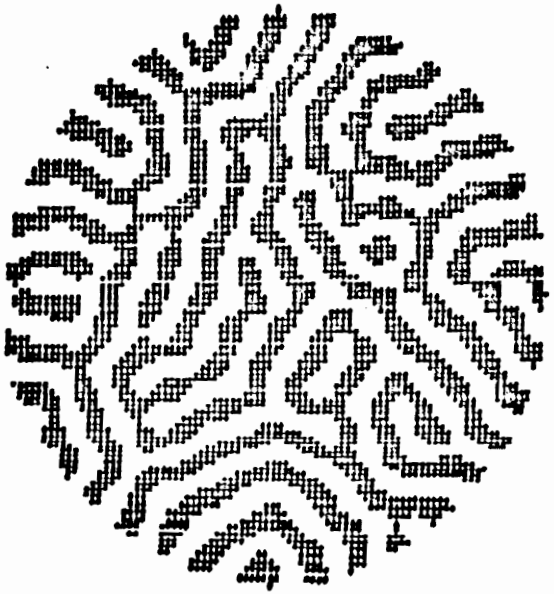

FIGURE 3

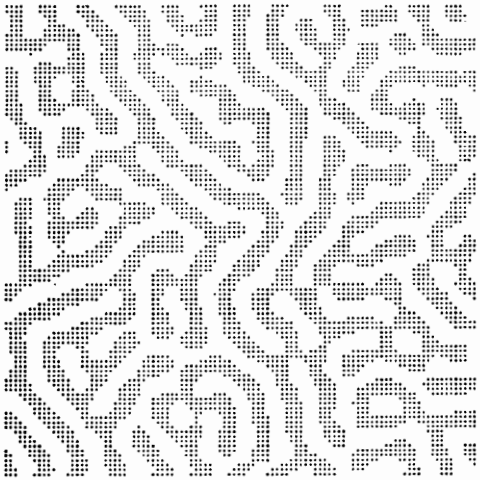

FIGURE 4

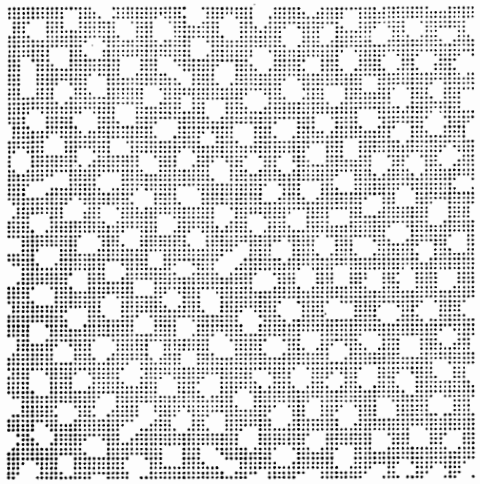

FIGURE 5

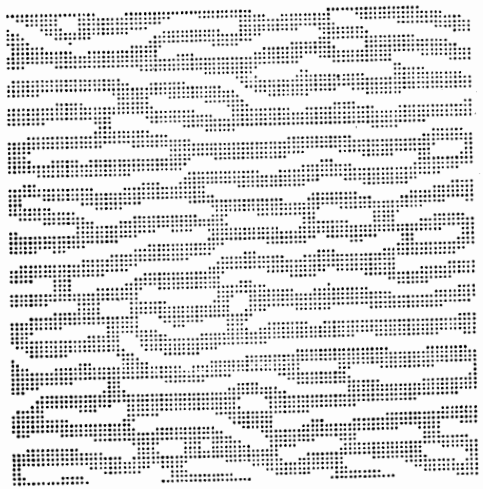

FIGURE 6